# UIDE

Powered by
**Arizona State University**

## ING. MECATRÓNICA

**Thesis prior to obtaining the degree of Mechatronics Engineer.**

**AUTHOR:** Martín Felipe Tobar Flores

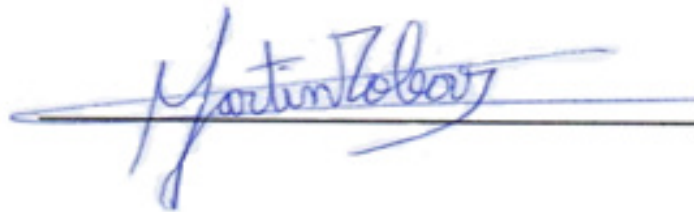**TUTOR:** Ing. Gabriela Andaluz, MSc.

Design and Implementation of an Electroencephalograph Prototype for the Acquisition and Visualization of Brain Signals which by Means of Neural Networks allows the Detection of an Anomaly

**QUITO – ECUADOR | 2023**

# CERTIFICATE OF AUTHORSHIP

I, MARTIN FELIPE TOBAR FLORES, hereby declare that this submission is my own work, it has not been previously submitted for any degree or professional qualification and that the detailed bibliography has been consulted.

I transfer my intellectual property rights to the Universidad Internacional del Ecuador, to be published and divulged on the internet, according to the provisions of the Ley de Propiedad Intelectual, its regulations and other legal dispositions.

**MARTIN FELIPE TOBAR FLORES**

# ACKNOWLEDGMENTS

To my parents Bayardo and Maritza, who have supported, cheered and advised me uncountable times troughout my whole life.

To my girlfriend María Elena who has supported, cheered and advised me these 9 semesters.

To my tutor MSc. Gabriela Andaluz for her advise and guidance.

To all my professors for the knowledge transferred and advise given along these 9 semesters.

# CONTENTS

# LIST OF FIGURES

# LIST OF TABLES

# MECHATRONICS DESIGN AND MATERIALS SELECTION

## 1. Structure alternative selection

### 1.1. Alternative 1

The alternative 1 is a structure similar to a serum holder. It consists of a mobile chair base with a steel bar/pipe as an axis which holds the EEG machine and with a table on mid stick to put a laptop on it. Fig. 1 shows a very similar idea but alternative 1 would have a table instead of a basket.



**Figure 1.** Alternative 1 [1].

### 1.2. Alternative 2

Alternative 2 is a 2-floor structure with 4 wheels, a side basket and a mobile EEG support. A better representation can be seen on Fig. 2 but considering that alternative 2 would not have the small shelf nor the keyboard space.



**Figure 2.** Alternative 2 [2].

## 1.3. Alternative 3

Alternative 3 which can be seen in Fig. 3 is a 2 floor, 4-wheeled mobile structure which has the EEG placed on top of the second floor on a fixed base. First floor can be used to put anything process-related such as creams/gels. It also has a hook to hold/support the EEG electrodes when the machine is not being used.
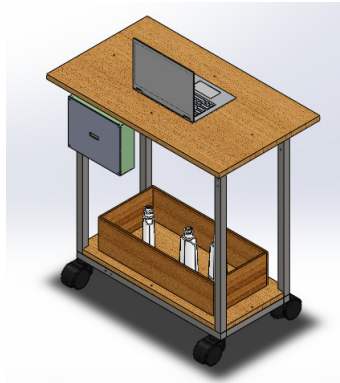


**Figure 3.** Alternative 3.

## 1.4. Criteria Description

The criteria used to choose the alternative is explained below and their ponderation can be seen in Table 1.

- **Aesthetics:** It is the visual quality of the design; it is important because it is the first thing the user see and it must make the user feel comfortable and satisfied.

- **Reliability:** It measures "how much can the machine be trusted". In this case it must assure that the components will not fall-off by even slipping or by mechanical failure (armature breaks and everything falls down). In this case it is the most important characteristic that is why it has the biggest ponderation weight.

- **Cost:** It is how much money it takes to build the design, it is important because in engineering the cost must be optimized as much as possible without compromising other factors such as resistance or reliability.

- **Building Complexity:** How hard it is to build the machine. It is important because on engineering time must be optimized and the least complex design should be chosen if it can fulfill the requirements.

- **Mobility:** The ability to move. It is important because the structure is mobile and should allow a smooth as possible movement without jamming or causing problems. Because this is the main feature/objective of the structure, it has a big ponderation weight (2nd biggest).

**Table 1.** Ponderation of each criteria used to choose which alternative is the most optimal one.

|  | Aesthetics | Reliability | Cost | Building Complexity | Mobility | Total |
|---|---|---|---|---|---|---|
|  | 0.2 | 0.3 | 0.15 | 0.1 | 0.25 | 10 |
| **Design 1** | 8 | 7 | 7 | 6 | 10 | 7.85 |
| **Design 2** | 8 | 10 | 4 | 7.5 | 10 | 8.45 |
| **Design 3** | 9 | 10 | 6 | 9 | 10 | 9.1 |

As it can be seen, the best grade was achieved by design 3, therefore it is chosen because it has the best overall aesthetics, reliability, cost, mobility and least building complexity. Furthermore it can be seen that it has space not only for a medium laptop, but for other things on both top and on bottom desks.

## 2. Mechanical Design

### 2.1. Desk dimensioning

The average height of people in Ecuador is $1.62\,\mathrm{m}$ [3], [4]. A recommended desk height for that average is: $59\,\mathrm{cm}$ to $63\,\mathrm{cm}$ [5], [6]. The average dimension of a laptop desk is $50\,\mathrm{cm}$ to $60\,\mathrm{cm}$ length and $30\,\mathrm{cm}$ to $40\,\mathrm{cm}$ width [7], [8] (the thickness will be selected further based on stress analysis). The table must be able to bear the weight of a person that is in the process of standing up or using the table as a support. There is no information in the state of art about this parameter, but an experiment was made to determinate an estimate value.

The weight of a person is measured once while standing up and once while supporting himself on the desk by using a balance. The difference in the measures mentioned is

the amount of force the person is exerting on the desk to support himself. The weight of the person was $686.7\,\mathrm{N}$ $(70\,\mathrm{kgf})$ and the weight measured when supporting himself was $491\,\mathrm{N}$. To find what is the exerted force in the desk:

$$F_e = W_p - W_m \tag{1}$$

Where:

$F_e$ is the exerted force, in $\mathrm{N}$;

$W_p$ is the person weight, in $\mathrm{N}$;

$W_m$ is the measured weight, in $\mathrm{N}$.

$$F_e = 686.7 - 491$$

$$F_e = 195.7\,\mathrm{N}$$

To find the exerted force as a percentage of the total weight of the person:

$$W_{per} = \frac{F_e}{W_p} \tag{2}$$

Where:

$W_{per}$ is the percentage weight that the table support, in $\%$.

$$W_{per} = \frac{195.7}{686.7}$$

$$W_{per} = 28\,\%$$

The average weight of Ecuadorian people is between $697\,\mathrm{N}$ to $726\,\mathrm{N}$ [3], [9] using the maximum average value found, it can be said that the average force exerted on the

desk by Ecuadorian people would be:

$$F_{EE} = W_E \cdot W_{per} \tag{3}$$

Where:

$F_{EE}$ is the average exerted force by an Ecuadorian, in $\mathrm{N}$;

$W_E$ is the average Ecuadorian weight, in $\mathrm{N}$.

$$F_{EE} = 726 \cdot 28$$

$$F_{EE} = 203.28\,\mathrm{N}$$

As it can be seen, the average exerted force should be $203.28\,\mathrm{N}$ which equals $20.7\,\mathrm{kgf}$, As this is an experimental found value, it is not exact and might to be safer the design is going to be made to support a force of $295\,\mathrm{N}$ which equals $30\,\mathrm{kgf}$, to have an error margin of $45\,\%$.

## 2.2. Table desk design

### 2.2.1. Desk Material selection

The desk can be made of multiple materials such as tempered glass, metal sheet and melaminic or lyaminated Wood. To select which of them is the optimal one a ponderation was done and can be seen on Table 2. The parameters used are:

- **Aesthetics:** It is the visual quality of the design; it is important because it is the first thing the user see and it must make the doctor and patient to feel comfortable and satisfied.

- **Resistance:** It is the ability of the material to have a long term duration and not break (mechanical resistance which is the most important) nor damage too soon (resistance to wear and tear).

- **Cost:** The amount of money needed to manufacture or process the material (which is reflected in the final price). This parameter needs to be as low as possible without compromising other factors such as resistance.

- **Cleanability** The ability of the material to be cleaned (how easy). This is important because as it will be in a medical office it must be easy to clean as asepsis is needed.

On Fig. 4 desks made of the selected materials can be seen. (The left wood table is melaminic and the right one is laminated).
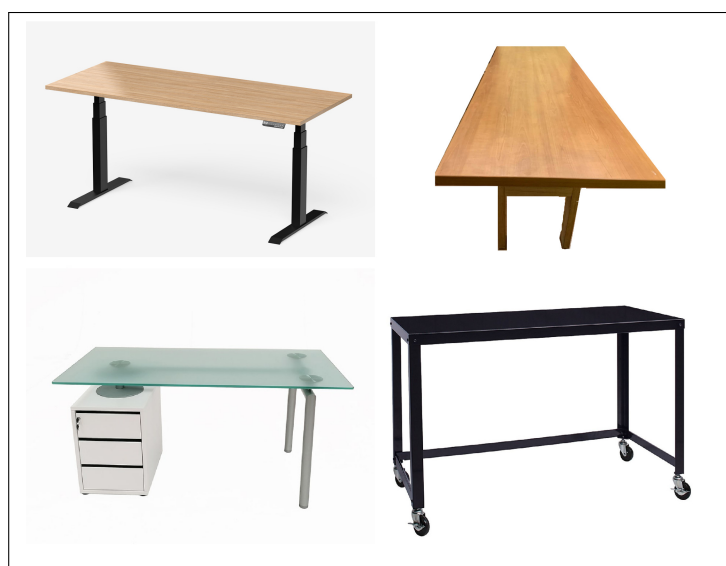


**Figure 4.** Desks made of different materials.

**Table 2.** Desk material ponderation table used to select which material is the most optimal one.

|  | Aesthetics | Resistance | Cost | Cleanability | Total |
|---|---|---|---|---|---|
| **Weight** | 0.2 | 0.4 | 0.2 | 0.2 | 10 |
| **Melaminic** | 10 | 9.5 | 9 | 10 | 9.6 |
| **Tempered Glass** | 7 | 9 | 4 | 10 | 7.8 |
| **Laminate** | 10 | 10 | 6 | 10 | 9.2 |
| **Metal Sheet** | 9 | 10 | 2 | 8 | 7.8 |

As it can be seen in Table 2, the best grade was achieved by melaminic wood, which has the best overall aesthetics, resistance, cost and cleanability making it the most adequate choice for being the desk table material. Therefore it is selected.

### 2.2.2. Cantilever Bending Stress Calculations

In the Ecuadorian market, there are 2 widths of melaminic: $15$ and $25\,\mathrm{mm}$ therefore, the calculus will be made for both to find which one is suitable.

The maximum bending stress formula is given by:

$$\sigma_b = \frac{M \cdot c}{I} \tag{4}$$

Where:

$\sigma_b$ is the bending stress, in $\mathrm{Pa}$;

$M$ is the moment, in $\mathrm{Nm}$;

$c$ is the distance from the neutral axis to the base, in $\mathrm{m}$;

$I$ is the moment of inertia, in $\mathrm{m}^4$.

Table 3 shows melaminic's important properties for bending calculation.

The graph of force, shear force and bending for a punctual load in cantilever can be seen on Fig. 5 from which it can be found out that:

$$M_{maxc} = P \cdot L_c \tag{5}$$

Where:

$M_{maxc}$ is the maximum bending stress in cantilever, in $\mathrm{Nm}$;

$P$ is the punctual load, in $\mathrm{N}$;

$L_c$ is the length of the beam in cantilever, in $\mathrm{m}$.

As it can be seen in Fig. 3, the desk has a cantilever between the upper desk edge and the steel structure. The distance that is in cantilever is $6\,\mathrm{cm}$. Therefore, replacing (5) in (4) it is found out that:

$$\sigma_{bc} = \frac{P \cdot L_c \cdot c}{I} \tag{6}$$

**Table 3.** Melaminic properties where the $15$ subindex corresponds to the $15\,\mathrm{mm}$ melaminic and $25$ corresponds to the $25\,\mathrm{mm}$ melaminic.

| Yield strength [10] <br><br> $\mathrm{MPa}$ | 24 |
|---|---|
| **Distance from neutral axis** $c_{15}$ <br><br> mm | 7.5 |
| **Distance from neutral axis** $c_{25}$ <br><br> mm | 12.5 |
| **Moment of inertia** $I_{15}$ <br><br> $\mathrm{mm}^4$ | 4218.75 |
| **Moment of inertia** $I_{25}$ <br><br> $\mathrm{mm}^4$ | 32552.08 |
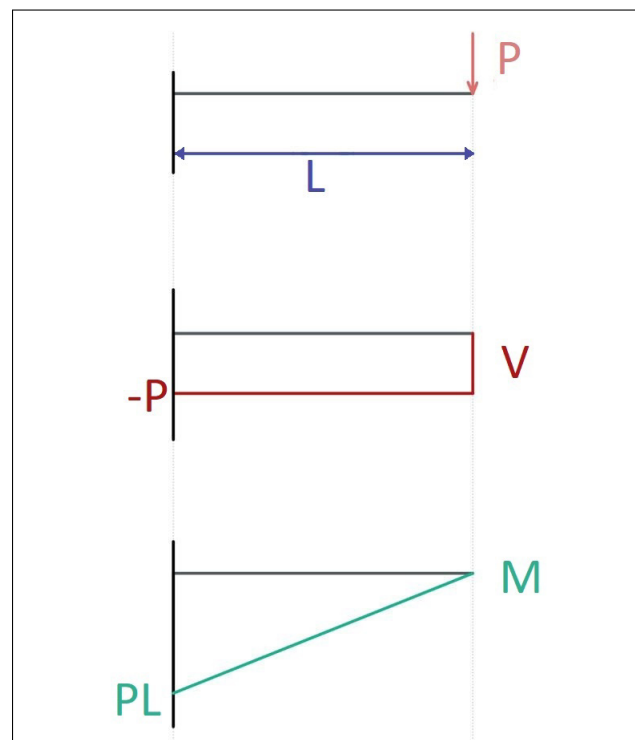


**Figure 5.** Shear force and momentum diagram for a punctual load in cantilever [11].

Where:

$\sigma_{bc}$ is the cantilever bending stress of the melamine, in $\mathrm{Pa}$.

Replacing (6) with the properties shown in Table 3 and with the punctual load found out at the end of section 2.1 for the $15\,\mathrm{mm}$ and $25\,\mathrm{mm}$ melaminic respectively:

$$\sigma_{bc15} = \frac{295 \cdot 0.06 \cdot 0.075}{4.218 \cdot 10^{-9}} = 31.47\,\mathrm{MPa} \tag{7}$$

Where:

$\sigma_{bc15}$ is the cantilever bending stress of the $15\,\mathrm{mm}$ melamine, in $\mathrm{Pa}$.

$$\sigma_{bc25} = \frac{295 \cdot 0.06 \cdot 0.125}{3.255 \cdot 10^{-8}} = 6.80\,\mathrm{MPa} \tag{8}$$

Where:

$\sigma_{bc25}$ is the cantilever bending stress of the $25\,\mathrm{mm}$ melamine, in $\mathrm{Pa}$.

The factor safety formula [12] is given by:

$$sf = \frac{\sigma_y}{\sigma_a} \tag{9}$$

Where:

$\sigma_y$ is the yield stress, in $\mathrm{Pa}$;

$\sigma_a$ is the applied stress, in $\mathrm{Pa}$.

Replacing (7) and (8) respectively in (9) and using the yield stress shown in Table 3 it is found out that:

$$sf_{15} = \frac{31.47}{24} = 0.6 \tag{10}$$

Where:

$sf_{15}$ is the safety factor of the $15\,\mathrm{mm}$ melamine, adimensional.

$$sf_{25} = \frac{6.8}{24} = 3.5 \tag{11}$$

Where:

$sf_{25}$ is the safety factor of the $25\,\mathrm{mm}$ melamine, adimensional.

Therefore the $25\,\mathrm{mm}$ melaminic will be used as the $15\,\mathrm{mm}$ melaminic will fail.

### 2.2.3.  Double support bending stress

As it was shown in section 2.2.2, the $15\,\mathrm{mm}$ melaminic is not suitable, therefore in this section the calculations will be done only for the $25\,\mathrm{mm}$ melaminic to demonstrate it will withstand the load applied.

The graph of force, shear force and bending for a punctual load in the middle of two supports can be seen on Fig. 6 from which it can be found out that:

$$M_{max2s} = \frac{P \cdot L_{2s}}{4} \tag{12}$$

Where:

$M_{max2s}$ is the maximum bending moment, in $\mathrm{Nm}$;

$L_{2s}$ is the length of the supported beam, in $\mathrm{m}$.

By replacing (12) in (4) the bending moment stress for this specific case is given by:

$$\sigma_{b2s} = \frac{P \cdot L_{2s} \cdot c}{4 \cdot I} \tag{13}$$

Where:

$\sigma_{b2s}$ is the melaminic maximum bending stress in 2 support configuration, in $\mathrm{Pa}$.

  The most critical distance is $48\,\mathrm{cm}$ because that is the longest distance between the supports holding the upper table. And then replacing (12) with with the properties of the $25\,\mathrm{mm}$ shown in Table 3 and with the punctual load found out at the end of section 2.1:

$$\sigma_{b2s} = \frac{295 \cdot 0.46 \cdot 0.125}{4 \cdot 3.255 \cdot 10^{-8}} = 13.03\,\mathrm{MPa} \tag{14}$$
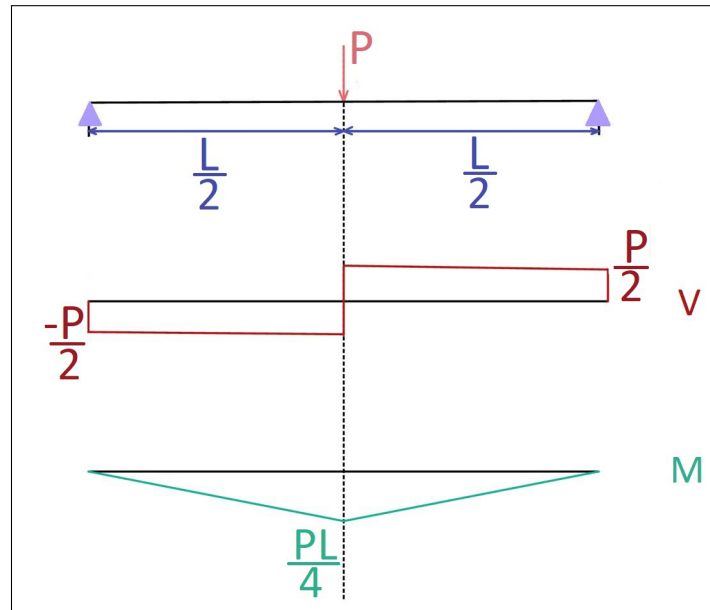
**Figure 6.** Shear force and momentum diagram for a punctual load in the middle of two supports [13].

To find the factor safety, (14) is replaced in (9) and using the yield stress shown in Table 3:

$$sf_{2s} = \frac{13.03}{24} = 1.8 \tag{15}$$

Where:

$sf_{2s}$ is the safety factor for the supported melaminic desk, adimensional.

Therefore, the $25\,\mathrm{mm}$ melaminic will not fail in this case either, so it can be used.

## 2.3. Inner Structure design

### 2.3.1. Inner Structure alternative selection

Because this is also a mechanical material selection, the same parameters that were considered for the desk material in section 2.2.1 are used for this section. On Fig. 7 the different materials proposed can be seen in the same order as on Table 4 which shows the ponderation to select the optimal one.

As it can be seen, the best grade is obtained by the steel square pipe which has the best overall aesthetics, resistance, cost and cleanability. Therefore it is chosen to be the support material.
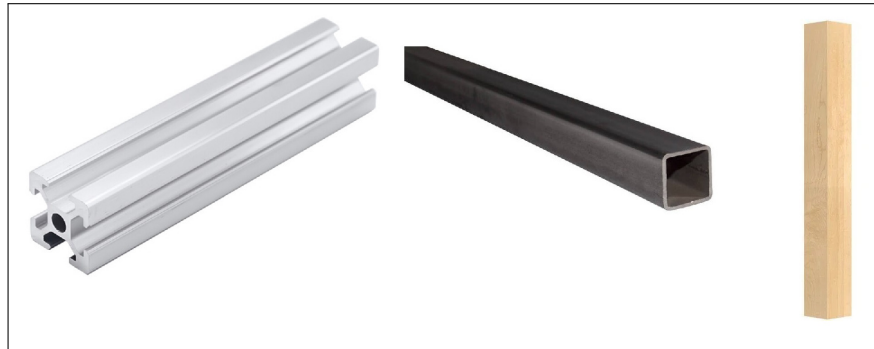
**Figure 7.** Proposed Support Materials.

**Table 4.** Support material ponderation table used to select which material is the most optimal one.

|  | Aesthetics | Resistance | Cost | Cleanability | Total |
|---|---|---|---|---|---|
| **Weight** | 0.1 | 0.5 | 0.3 | 0.1 | 10 |
| **Aluminum Profile** | 8 | 10 | 5 | 10 | 8.3 |
| **Steel square Pipe** | 9 | 10 | 9 | 10 | 9.6 |
| **Wood** | 6 | 8 | 9 | 10 | 8.3 |

### 2.3.2. Double support bending stress calculus

The cheapest standardized steel square pipe that can be found in the Ecuadorian market is the SAE J 403 1008 whose geometric characteristics can be seen in Fig. 8 and described in Table 5.
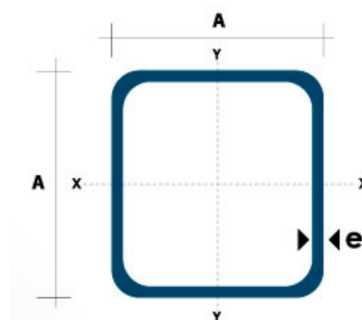


**Figure 8.** SAE J 403 1008 Steel square pipe dimension parameters image [14].

Table 6 shows steel's important properties for bending calculation.

**Table 5.** Parameters of the square tube [14].

| A | Width (e) | Weight | Area | Inertia momentum |
|---|---|---|---|---|
| mm | mm | kg/m | cm$^2$ | cm$^4$ |
| 20 | 1.2 | 0.72 | 0.9 | 0.53 |

**Table 6.** Steel pipe properties used for bending stress calculation.

| | |
|---|---|
| **Yield strength [15]** <br><br> MPa | 285 |
| **Distance from neutral axis** $c_s$ <br><br> mm | 10 |
| **Moment of inertia** $I_s$ **[14]** <br><br> cm$^4$ | 0.53 |

The maximum bending stress formula for this case is is given by:

$$\sigma_{bs} = \frac{M_s \cdot c_s}{2 \cdot I_s} \tag{16}$$

Where:

$\sigma_{bs}$ is the bending stress in each steel pipe, in $\mathrm{Pa}$;

$M_s$ is the steel pipe moment, in $\mathrm{Nm}$;

$c_s$ is the steel pipe distance from the neutral axis to the base, in $\mathrm{m}$.

Notice that is the same as (4) but as in this case there are 2 tubes supporting the punctual load, the stress in each tube, will be half of the total stress.

Replacing (12) in (16) it is found out that:

$$\sigma_{bs} = \frac{P \cdot L_s \cdot c_s}{2 \cdot I_s} \tag{17}$$

Where:

$L_s$ is length of the steel pipe supported beam, in $\mathrm{m}$.

Replacing (17) with the properties of the steel pipe shown in Table 6 and with the punctual load found out at the end of section 2.1:

$$\sigma_{bs} = \frac{295 \cdot 0.46 \cdot 0.1}{2 \cdot 5.337 \cdot 10^{-9}} = 31.78\,\text{MPa} \tag{18}$$

To find the safety factor replace (18) in (9) and using the yield stress shown in Table 6:

$$sf_s = \frac{31.78}{285} = 8.97 \tag{19}$$

Where:

$sf_s$ is the safety factor for the steel bending stress, adimensional.

Therefore it can be concluded that this steel pipe tube is suitable for supporting this bending stress.

### 2.3.3. Buckling Calculus

The most critical case for buckling force is when there is a cantilever configuration. The punctual load will be applied in the upper table which is free to move. The lower part of the desk will be held in place by the blocked wheels, therefore it can be analyzed as a cantilever configuration. The formula to find the maximum allowed buckling force in cantilever is:

$$F_{max} = \frac{\pi^2 \cdot E_s \cdot I_s}{4 \cdot L_{buck}^2} \tag{20}$$

Where:

$F_{max}$ is the maximum allowed force per steel pipe, in $\text{N}$;

$E_s$ is the steel pipe elastic modulus, in $\text{Pa}$;

$I_s$ is the steel pipe moment of inertia, in $\text{m}^4$;

$L_{buck}$ is the steel pipe length in cantilever for buckling, in $\text{m}$.

The steel pipe elastic modulus $E_s$ is $200\,\text{GPa}$ [15] the steel pipe moment of inertia $I_s$ is $0.53\,\text{cm}^4$ [14] and the cantilever length for buckling $L_{buck}$ is $50\,\text{cm}$. Replacing this values

in (20):

$$F_{max} = \frac{\pi^2 \cdot 200 \cdot 10^9 \cdot 0.5337 \cdot 10^{-9}}{4 \cdot 0.5^2} = 10.5 \,\text{kN} \qquad (21)$$

As it can be seen, the maximum allowed buckling force is much higher than the nominal force found at the end of section 2.1 but is still desired to find the safety factor.

The force safety factor is given by:

$$sf_f = \frac{F_{ma}}{F_a} \qquad (22)$$

Where:

$sf_f$ is the force safety factor, adimensional.

$F_{ma}$ is the maximum allowed force, in $\text{N}$.

$F_a$ is the applied force, in $\text{N}$.

The working force in this case is the nominal force divided by 4 because there are 4 columns (steel pipes) that together bear the whole load. Therefore replacing the values in (22): The force safety factor is given by:

$$sf_f = \frac{4 \cdot 10500}{295} = 143 \qquad (23)$$

## 2.4. Wheels selection

For the wheels, 4 of them are going to be used and it only is needed that they are able to support the force exerted on the desk which was found at the end of section 2.1 and that they can be blocked or unblocked manually. Therefore the wheel selected and that can withstand up to $30 \,\text{kg}$ each [16] can be seen on Fig. 9.



**Figure 9.** Wheel selected that has a manual block [16].

## 3.  Electronic design

The electronic design consists in selecting and designing the electronic elements that are going to be used in the prototype.  The circuit is composed by some elements which are a microcontroller, an amplifier, an anti alias filter and the electrodes.  These elements can be seen in the block diagram shown in Fig. 10
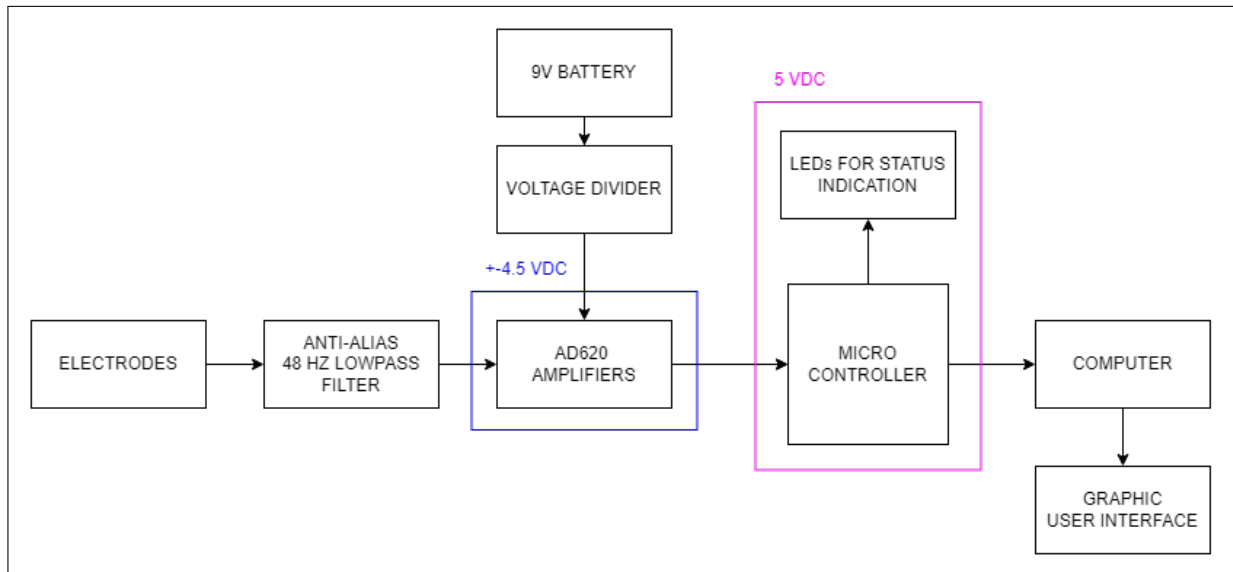


**Figure 10.** Electronic circuit block diagram.

## 3.1.  Electrodes selection

Electrodes are a very important component because they are the elements that capture the electroencephalographic waves. There are two types of electrodes mainly, wet and dry electrodes. The difference is that wet electrodes need a conductive gel to work and dry do not.  Due to this reason, dry electrodes are not so good as wet electrodes as they are more likely to be affected by noise and motion artifacts unless the experiment is done in a stationary way.  In this case, both will have a high performance but wet electrodes will be slightly higher [17]. The ponderation for the electrodes can be seen on Table 7, where the "Application" column stands how good the electrodes are for a stationary application (as is this case).

**Table 7.** Electrodes ponderation table used to select which type of electrode is the most optimal one.

|  | Cost | Quality | Application | Time to mount | Total |
|---|---|---|---|---|---|
| **Weight** | 0.2 | 0.3 | 0.3 | 0.2 | 1 |
| **Dry electrode** | 10 | 7.5 | 8 | 10 | 8.65 |
| **Wet electrode** | 10 | 9 | 9 | 6 | 8.6 |

## 3.2. Filter design

The acquired signal must go through a series of filters to eliminate noise that is not part of the brainwaves, this is illustrated with a block diagram which is shown in Fig. 11. The minimum low-pass filtered generally used for EEG is $30\,\mathrm{Hz}$ [18], [19] the American
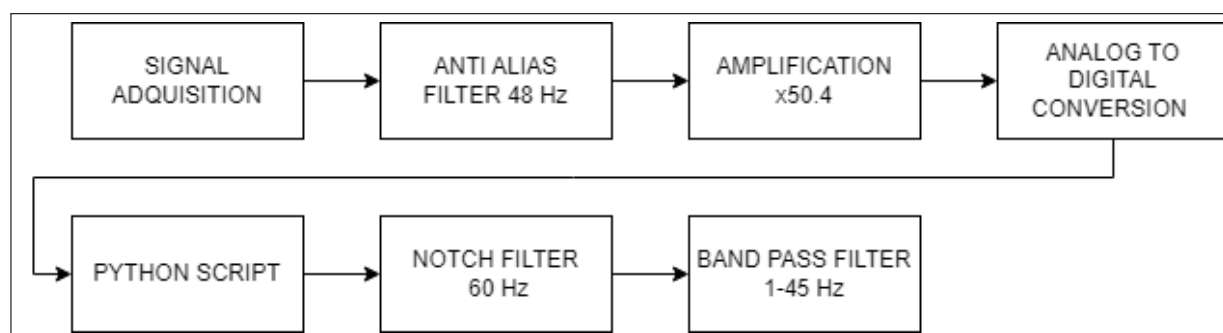


**Figure 11.** Signal filtering diagram blocks.

Clinical Neurophysiology Society recommends at least $35\,\mathrm{Hz}$ [20] as the low-pass filter threshold. The problem with this filtering is that it eliminates the Gamma band but this is done because this band is not widely used in researching [21]. Nowadays, the software filters are heavily preferred over the hardware filters because they are cheaper, do not occupy physical space, can be changed easily, are more powerful and are not affected by external factors such as aging and temperature [22]. Even though as it has been shown, there are several advantages of software filters over hardware filters, at least an anti-aliasing filter should be implemented physically. The frequency cut chosen is $45\,\mathrm{Hz}$ because gamma band is desired to be included and the common upper limit to research this frequency is around this value [21]. Also, in the artificial intelligence state of art for epilepsy some research as [23] use $45\,\mathrm{Hz}$ as the low-pass filter cut-off

frequency value. A simple low-pass filter can be seen in Fig. 12.

The cutoff frequency formula is given by:
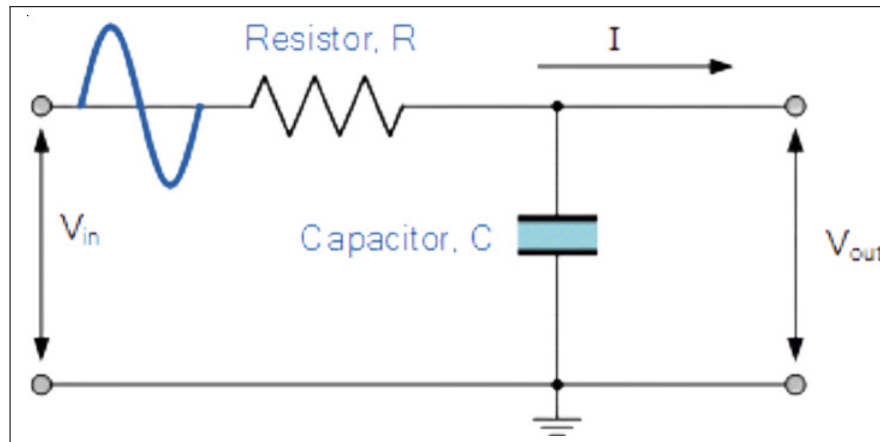


**Figure 12.** Simple low-pass filter configuration [24].

$$f_{cut} = \frac{1}{2 \cdot \pi \cdot R_f \cdot C_f} \tag{24}$$

Where:

$f_{cut}$ is the cut off frequency, in $\mathrm{Hz}$;

$R_f$ is the resistance used for the low-pass filter, in $\Omega$;

$C_f$ is the capacitor used for the low-pass filter, in $\mathrm{F}$.

In this case, the cut frequency is $45\,\mathrm{Hz}$ and typically to design a low-pass filter the resistance value is based on the capacitor value which is chosen first because commercially there are more resistance values than capacitors, hence it is easier to find a suitable resistor for a given capacitor.

Therefore by selecting a capacitor of $100\,\mu\mathrm{F}$ the resistance can be found by:

$$R_f = \frac{1}{2 \cdot \pi \cdot f_{cut} \cdot C_f} \tag{25}$$

$$R_f = \frac{1}{2\pi \cdot 45 \cdot 100 \cdot 10^{-6}} = 35.36\,\Omega$$

The closest commercial resistance suitable for this is $33\,\Omega$. To see what is going to be

the real cut off frequency, this value is replaced in (24):

$$f_{cr} = \frac{1}{2 \cdot \pi \cdot 33 \cdot 100 \cdot 10^{-6}} = 48\,\mathrm{Hz} \qquad (26)$$

Where:

$f_{cr}$ is the real-cut off frequency, in $\mathrm{Hz}$.

Finally, it can be remarked that another advantage of the designed filter is that it will attenuate the $60\,\mathrm{Hz}$ power line wave before it goes intro the amplifier. Furthermore, a notch filter of $60\,\mathrm{Hz}$ is applied by software as well as a pass-band filter that goes from to $1\,\mathrm{Hz}$ to $45\,\mathrm{Hz}$ which is implemented with the M.N.E. python library for the EEG recording [25]. An example of the notch filter behavior can be seen in Fig. 13 and an example of a pass-band filter behavior can be seen in Fig. 14.
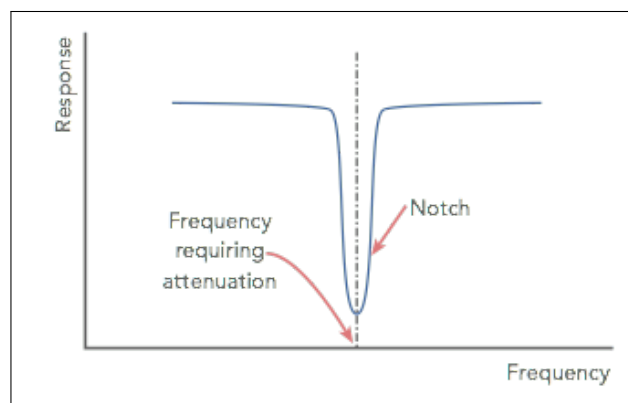


**Figure 13.** Notch filter behavior [26].

## 4. Amplification stage design

For the amplification stage, the AD620 high accuracy instrumentation amplifier was selected. It needs only 1 resistor to set a gain in the range of x1 to x10000. It has low noise and low bias current makes it suitable for medical equipment applications [28]. Among its applications:

- Weigh scales.

- ECG, EEG and medical instrumentation.

- Data acquisition system.
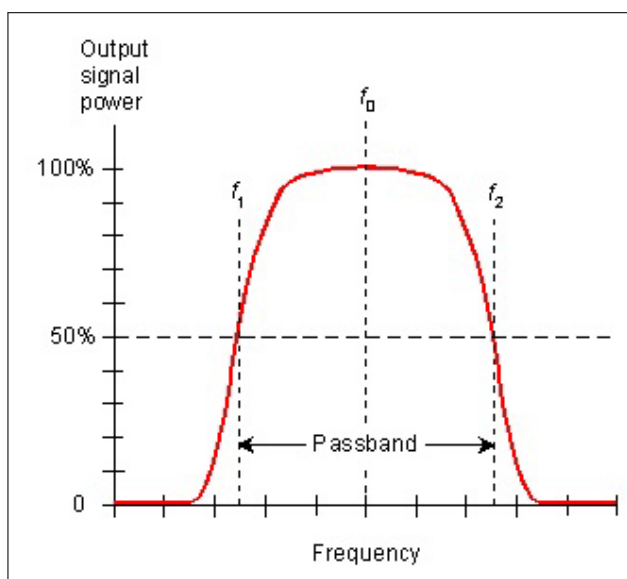
**Figure 14.** Bandpass filter behavior [27].

- Battery-powered and portable equipment.

The AD620 main features can be seen in Table. 8, its maximum ratings can be seen in Table 9, its schematic diagram can be seen in Fig. 15 and the AD620 configuration used for this prototype can be seen in Fig. 16.

**Table 8.** AD620 features [28].

| FEATURE | VALUE |
|---|---|
| Easy to use | |
| Gain set with one external resistor | |
| Gain range | 1 - 10000 |
| Power supply range | $\pm 2.3\,\text{V}$ to $\pm 18\,\text{V}$ |
| Higher performance than 3 op amp IA designs | |
| Available in 8-lead DIP and SOIC packaging | |
| Low power, 1.3 mA max supply current | |
| Input offset voltage | $50\,\mu\text{V}$ |
| Settling time to 0.01% | $15\,\mu\text{s}$ |
| Low noise | |

**Table 9.** AD620 maximum rating values [28].

| Parameter | Rating |
|---|---|
| **Supply Voltage** | $18\,\text{V}$ |
| **Internal Power Dissipation** | $650\,\text{mW}$ |
| **Input Voltage (Common-Mode)** | Vs |
| **Differential Input Voltage** | $25\,\text{V}$ |
| **Output Short-Circuit Duration** | Indefinite |
| **Storage Temperature Range (Q)** | $-65\,^{\circ}\text{C}$ to $150\,^{\circ}\text{C}$ |
| **Storage Temperature Range (N, R)** | $-65\,^{\circ}\text{C}$ to $125\,^{\circ}\text{C}$ |
| **Operating Temperature Range** | $-40\,^{\circ}\text{C}$ to $85\,^{\circ}\text{C}$ |
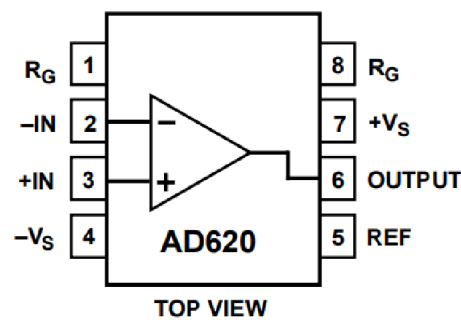


**Figure 15.** AD620 instrumental amplifier schematic diagram [28].

To find the gain used, the AD620 amplification formula is used which is given by:

$$G = \frac{49400}{R_g} + 1 \tag{27}$$

Where:

$G$ is the Gain of AD620, in adimensional;

$R_g$ is the gain resistance, in $\Omega$.

As a $1\,\text{k}\Omega$ gain resistor was used, the obtained gain is:

$$G = \frac{49400}{1000} + 1 = 50.4 \tag{28}$$
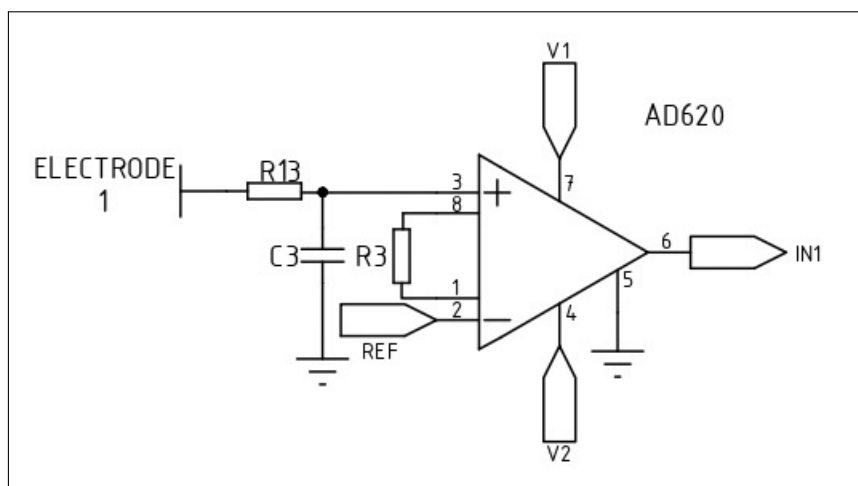
**Figure 16.** AD620 schematic diagram of the configuration used.

Finally, it can be concluded that for the amplification stage was designed by using an AD620 amplifier which is fed with $\pm\,4.5\,\mathrm{V}$ and that has a $50.4\,\mathrm{x}$ gain applied to the voltage difference between an scalp electrode and the reference electrode.

## 4.1. Microcontroller selection

For the microcontroller selection, the most important features needed are the abilities to capture and digitize the brain waves and send them to a laptop that has the developed EEG software installed. For these reasons the selection of the microcontroller is based on ADC characteristics and serial communication features which are listed below and whose ponderation table can be seen on Table 10.

- **ADC channels:** Is the amount of channels (or input pins) able to digitize an analog signal. For AI applications for epilepsy detection the minimum amount of channels is 1 [29], [30].

- **ADC Resolution:** Is the smallest incremental voltage that is detected by the microcontroller. The higher the resolution, the higher the precision of the measurement. The minimum amount of ADC bits should be 10 bits to have a good waveform signal sampling [31], [32].

- **Cost:** Amount of money needed to purchase the microcontroller.

- **Sampling Frequency:** Is the amount of samples that the microcontroller is able to take in a second. The higher the sampling time, the better is reconstructed the measured analog input. According to nyquist theorem [33], the sampling rate should be at least twice the signal maximum frequency, and according to American Society Guideline [20], it is recommended to use a minimum sampling rate of $135\,\mathrm{Hz}$ for a $45\,\mathrm{Hz}$ high pass filtered EEG, which is the case of this prototype. Using this recommendation, and the amount of channels to be used (10) it can be found the minimum sample rate of the controller.

$$Fs_{min} = Ch_n \cdot Fs_{ch} \tag{29}$$

Where:

$Fs_{min}$ is the minimum required sampling rate, in $\mathrm{Hz}$;

$Ch_n$ is the number of channels;

$Fs_{ch}$ is the needed sampling rate per channel, in $\mathrm{Hz}$.

Replacing the values in (29):

$$Fs_{min} = 10 \cdot 135 = 1350\,\mathrm{Hz} \tag{30}$$

- **USART Baud Rate:** Amount of bits per second that the USART serial communication of the microcontroller is able to transfer. The higher the more information can be transferred in a period of time. In this case an overhead of 3 bits per byte (start bit, end bit and parity bit) will be used. Therefore, the minimum baudrate can be calculated as:

$$bpspl = 3 \cdot (\ B\ + Oh\ ) \tag{31}$$

Where:

$bpspl$ are the total units of data per sample, in $\mathrm{bps}$;

$B$ is a unit of data, in $\mathrm{B}$;

$Oh$ is the unit of data overhead, in $\mathrm{B}$.

$$bpspl = 3(8 + 3) = 33 \tag{32}$$

It is multiplied by 3 because to transfer the 10 bit ADC resolution sample, 2 bytes are needed and 1 extra byte is needed to encode the reading channel as a char, therefore 3 bytes are needed per channel. And to find what the minimum baudrate the microcontroller should have:

$$Bd_{min} = bpspl \cdot Fs_{min} \tag{33}$$

Where:

$Bd_{min}$ is the minimum required baudrate, in $\mathrm{Bd}$.

$$Bd_{min} = 33 \cdot 1350 = 44\,500\ Bd \tag{34}$$

**Table 10.** Microcontroller ponderation table used to select which is the most optimal one.

| | ADC channels | ADC Resolution | Cost | USART Baud Rate | Sampling frequency | Total |
|---|---|---|---|---|---|---|
| **Weight** | 0.15 | 0.3 | 0.15 | 0.2 | 0.2 | 1 |
| **PIC18F2550 [34]** | 10 | 8 | 9 | 8 | 10 | 8.85 |
| **RASP. PI [35]** | 0 | 0 | 3 | 10 | 10 | 4.45 |
| **ATMEGA2560 [36]** | 10 | 8 | 6 | 5 | 10 | 7.8 |

As it can be seen, PIC18F2550 was chosen. Among its main features it includes 10 ADC channels, a 10-bit resolution ADC and a maximum baudrate of 115200 $\mathrm{Bd}$. More of its features can be seen in Table 11 and its technical diagram can be seen in Fig. 17.
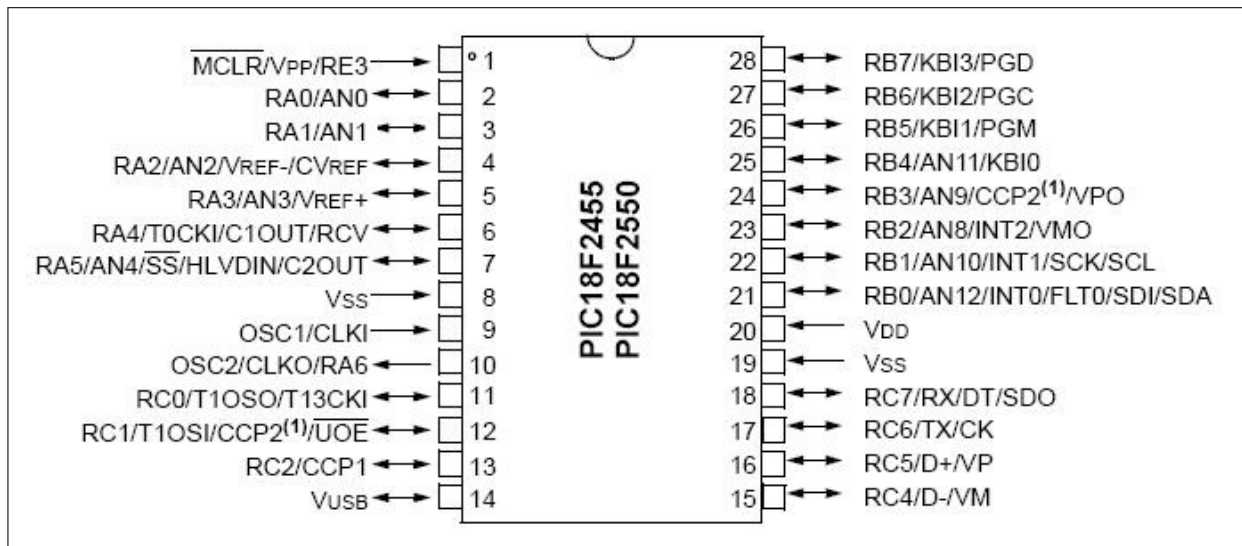
**Figure 17.** PIC18F2550 microcontroller schematic diagram [34].

**Table 11.** PIC18F2550 feature table summary [34].

| | |
|---|---|
| **Operating Frequency** | DC-48MHz |
| **Program Memory (Bytes)** | 32768 |
| **Program Memory (Instructions)** | 16384 |
| **Data Memory (Bytes)** | 2048 |
| **Data EEPROM Memory (Bytes)** | 256 |
| **Interrupt Sources** | 19 |
| **I/O Ports** | Ports A, B, C, (E) |
| **Timers** | 4 |
| **Capture/Compare/PWMModules** | 2 |
| **Enhanced Capture/ Compare/PWM Modules** | 0 |
| **Serial Communications** | MSSP, Enhanced USART |
| **Universal Serial Bus (USB) Module** | 1 |
| **10-Bit Analog-to-Digital Module** | 10 Input Channels |

## 4.2. Power supply design.

### 4.2.1. Design of $5\,\mathrm{V}$ source.

The total consumption of the prototype per source can be seen in Table 12 but this table does not take into account the power consumed by the computer because this will depend on the computer that is used (the computer is not part of the prototype and the user must use their own). USB 2.0 is able to provide up to $500\,\mathrm{mA}$ and USB 3.0 is able to provide up to $900\,\mathrm{mA}$ [37]. This transformed to power is $2.5\,\mathrm{W}$ and $4.5\,\mathrm{W}$ respectively. As it can be seen in Table 12, the total power consumption of the $5\,\mathrm{V}$ source is $0.7\,\mathrm{W}$, therefore any computer that has USB 2.0 or USB 3.0 is suitable to be used as the $5\,\mathrm{V}$ source.

### 4.2.2. Design of $9\,\mathrm{V}$ source.

As it can be seen in Table 12, the total current consumption of the $9\,\mathrm{V}$ source is $33\,\mathrm{mA}$. Therefore, for a 1 hour usage a battery with a capacity of $33\,\mathrm{mAh}$ is needed. Commercially, it is usual to find $9\,\mathrm{V}$ batteries with nominal capacities around $175\,\mathrm{mAh}$ such as the Energizer NH22-175 [38] which in this case would give an usage time of 5 hours and 18 minutes.

**Table 12.** Electronic consumption of the prototype without the computer power consumption.

| Element | Current $\mathrm{mA}$ | Power $\mathrm{W}$ |
|---|---|---|
| $5\,\mathrm{V}$ **COMPUTER** | | |
| PIC18F2550 | 100 | 0.5 |
| 2 LEDs | 40 | 0.2 |
| $9\,\mathrm{V}$ **BATTERY** | | |
| 10 AD620 | 13 | 0.117 |
| LED | 20 | 0.18 |
| Total | | 0.997 |

## 4.3. Signage Design

The prototype has 3 states which can be seen in Table 13 as well as how the LEDs are turned on or off to let the user know which is the current status of the prototype.

**Table 13.** LEDs indication for different states

| STATE | LED | | |
|---|---|---|---|
| | **GREEN** | **ORANGE** | **BLUE** |
| **USB CONNECTED** | OFF | ON | OFF |
| **PROTOTYPE ON** | OFF | ON | ON |
| **AMPLIFIERS ON** | ON | ON | ON |

## 4.4. Electronic design summary

A summary of the electronic elements used for this prototype can be seen in Table 14.

**Table 14.** Summary table of the selected electronic elements.

| ELEMENT | QUANTITY | MODEL/BRAND | CHARACTERISTICS |
|---|---|---|---|
| **CAPACITORS** | | | |
| 22pf CERAMIC | 2 | | 10V |
| 100uF ELECTROLYTIC | 11 | | 10V |
| **RESISTORS** | | | |
| 1k | 3 | | $\frac{1}{4}$ W |
| 1k | 10 | | $\frac{1}{4}$ W |
| 33 | 11 | | $\frac{1}{4}$ W |
| 220 | 5 | | $\frac{1}{4}$ W |

| ELEMENT | QUANTITY | BRAND | CHARACTERISTICS |
|---|---|---|---|
| **OTHERS** | | | |
| PIC18F2550 | 1 | Microchip | • 10 ADC channels 10 bit resolution.<br>• 115200 baudrate.<br>• USB serial communication.<br>• $5\,\text{V}$<br>• $100\,\text{mA}$ |
| AD620 | 10 | Analog Devices | • $50.4\,\text{x}$ Gain.<br>• Instrumental Amplifier.<br>• Used for EEG and ECG.<br>• Serial communication.<br>• $\pm 4.5\,\text{V}$<br>• $1.3\,\text{mA}$ |
| 20 MHz CRYSTALL | 1 | | |
| SWITCH | 2 | Gravitech | • Supports up to $10\,\text{A}\ 125\,\text{VAC}$.<br>• Simple Contact.<br>• Normally Opened.<br>• Rocker type. |
| LED | 3 | Farnell | • Indicator lights.<br>• 1 Green, 1 Orange, 1 Blue.<br>• $5\,\text{V}$<br>• $20\,\text{mA}$ |

## 5. Informatics Design

### 5.1. Programming language selection

The programming language is used to decode the bytes (codified brain waves) received by serial communication, process them (apply filters and data handling e.g. save them in EDF format), display the EEG signals in a GUI and apply a Deep Learning CNN binary classification algorithm to detect if there are epilepsy patterns. Also the knowledge on the programming language is taken in consideration as it can be translated to cost. (Less knowledge means more time and effort investment which increases the developing expenses). The ponderation for the programming language can be seen on Table 15.

**Table 15.** Language program ponderation table used to select which material is the most optimal one.

|          | EEG Modules | AI Modules | Serial Com. | GUI | Knowledge | Total |
|----------|-------------|------------|-------------|-----|-----------|-------|
| **Weight** | 0.3       | 0.3        | 0.2         | 0.1 | 0.1       | 1     |
| **Matlab** | 9         | 9          | 10          | 7   | 7         | 8.2   |
| **C++**    | 8         | 8          | 10          | 7   | 5         | 7.2   |
| **Python** | 9         | 10         | 10          | 7   | 8         | 8.8   |

### 5.2. Software development

The software which was developed using Python [39], Tkinter [40] and M.N.E [25], was made in such a way to make it as simple as possible for its user to utilize it. The application is composed of a main screen which can be seen in Fig. 18 which allows the user to choose between making a new recording, show a past recording or to make the epileptic analysis on a recording. If the user chooses the "MAKE EEG" option, the Maker screen which can be seen in Fig. 19 will appear. This screen allows the user to enter the patient's name, the doctor's name and to select the duration in seconds in intervals of $30\,\text{seconds}$. Once all the data is entered, the user must press start and the system will activate, the text will change to let the user the EEG is in progress and a
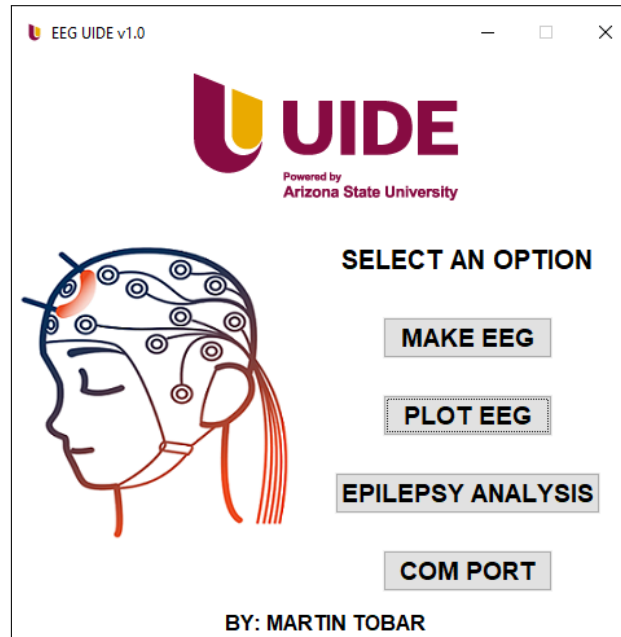
**Figure 18.** Main screen that appears when the software is opened up.

counter will begin as can be seen in Fig. 20. Also there is a pop-up notification to tell the user the recording is finished.
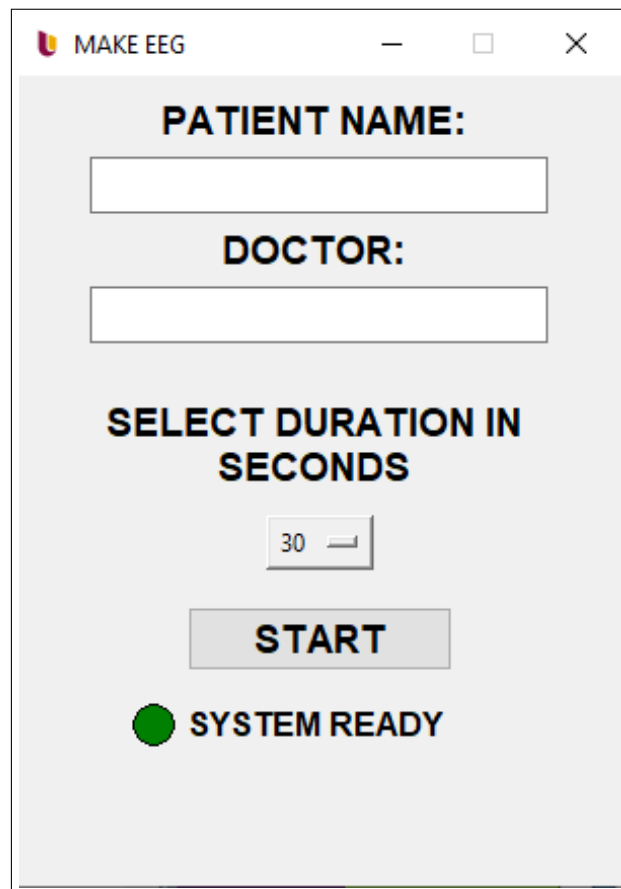


**Figure 19.** EEG recorder screen when opened up.

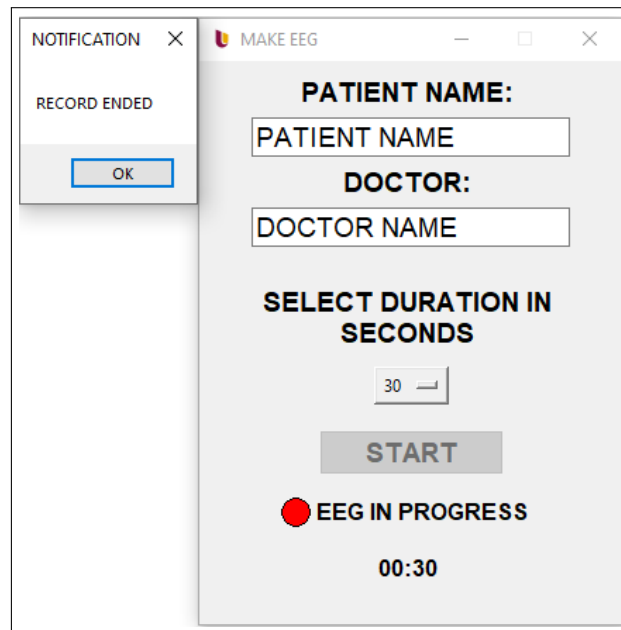If the user selects the "PLOT EEG" option, a file dialog will pop-up and let the user

**Figure 20.** Make screen that appears when the EEG recording is finished.

choose between EDF files. Once a file is chosen, a window will pop-up and allow the user to choose between plotting the whole recording along with its frequency spectrum. Also there is the option to export the EDF file in PDF format. All these features can be seen in Fig. 21. Finally, if the user selects the "Epilepsy Detection" option, a file dialog
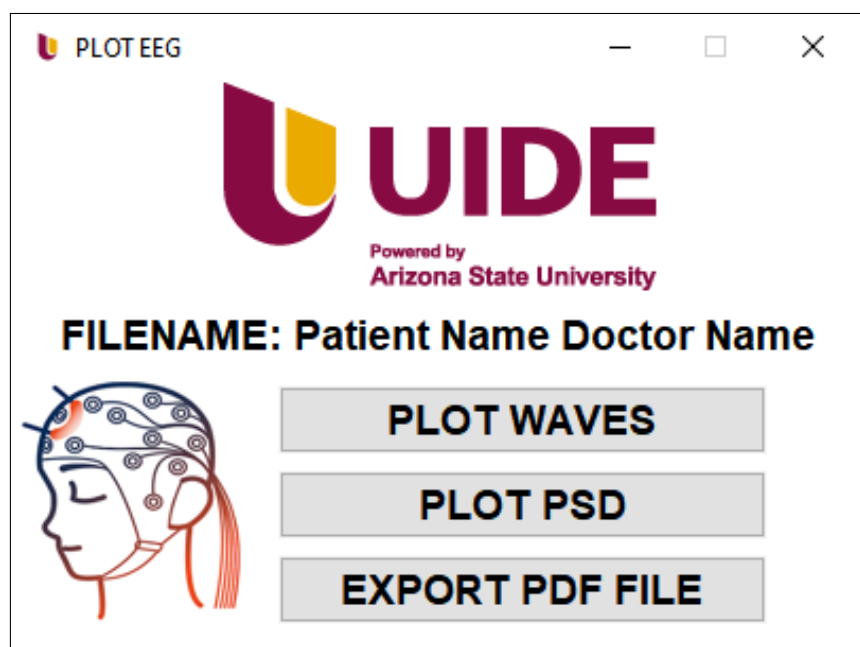


**Figure 21.** Screen that allows the user to choose between different plotting options.

will pop-up and let the user choose an EDF file in which the CNN binary classification algorithm will run. Once the EDF file is chosen and the classification is finished, a notification will pop-up and let the user know if this file contains epilepsy patterns or
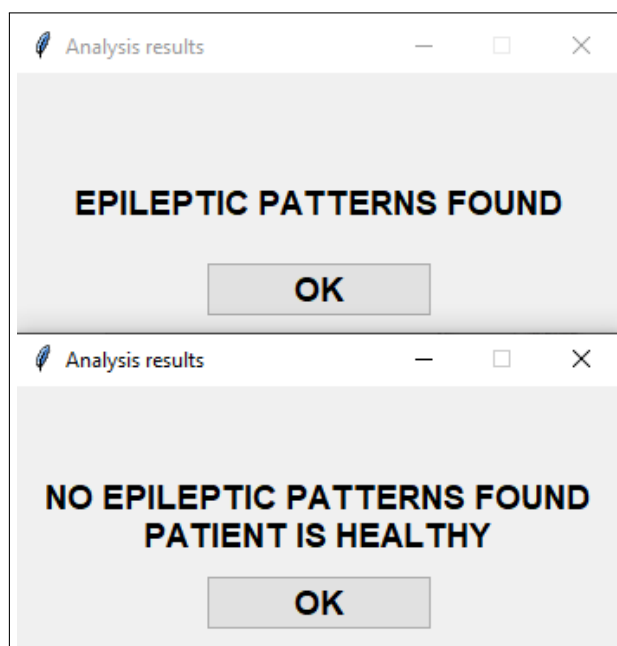
not. These notification can be seen in Fig. 22



**Figure 22.** Notification screens for epileptic patterns analysis result.

## 5.3. Convolutional Neural Network

A convolutional neural network (CNN) is a type of deep learning algorithm that is used for image and video recognition, signals processing, classification binary, autonomous driving, among others [41]. The architecture of a traditional neural network which can be seen in Fig. 23 is inspired in the brain whose operation relies in the connection of "nodes" which are the neurons and that are divided in 3 layers: input, hidden and output [42]. The difference between a generic neural network and a convolutional neural network, is that the convolutional neural network has a layer which makes a mathematical operation known as "convolution" whose main purpose is to find a feature inside a section of the input which is known as a kernel [43]. An architecture of a generic CNN can be seen in Fig. 24.

Some notable features and benefits of a CNN include [46]:

- To recognize and find patterns by themselves.

- Compress and reduce the dimensionality of the data that is given as an input by extracting its most important features.
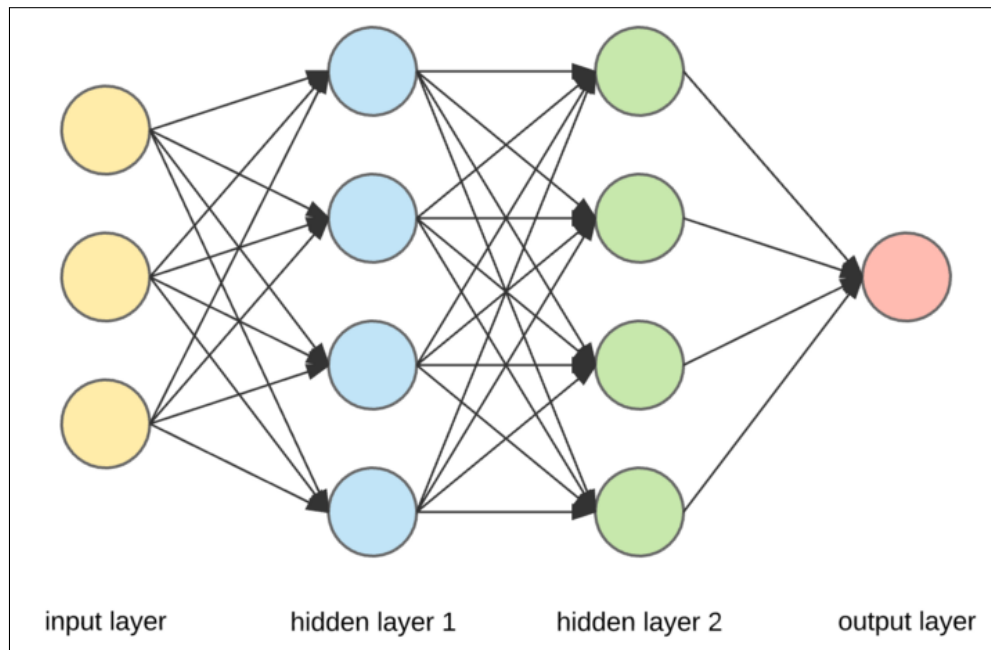
**Figure 23.** Generic neural network architecture [44].



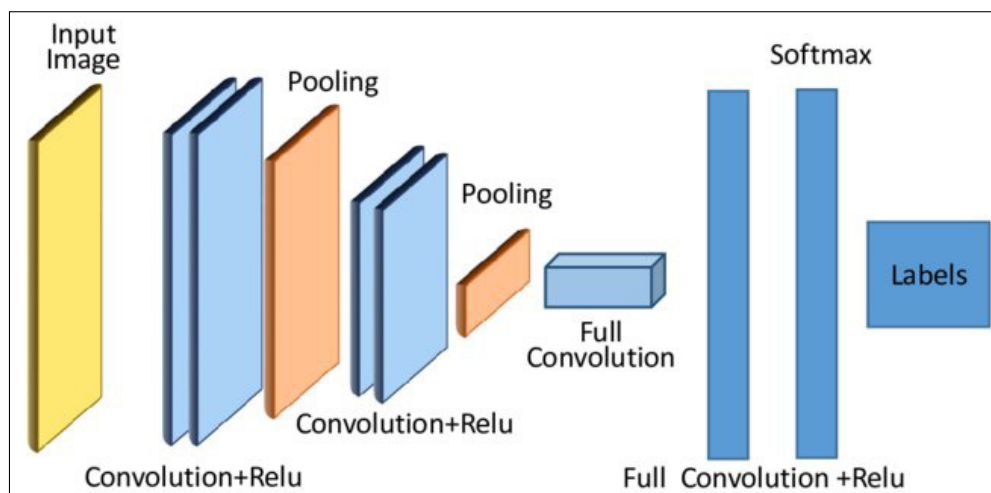**Figure 24.** Generic convolutional neural network architecture [45].

- It is computationally efficient.

- Are remarkable for classification.

- Work great for real time applications.

To summarize what each CNN layer does:

- **Convolution:** It makes a comparison to find feature inside a given input.

- **Pooling:** It syntethizes the information and reduces the dimensionality of the given input.

- **Linear Rectifier (Re-Lu):** It eliminate the negative values of the given input.

- **Fully connected:** Is the output layer of the CNN and is where the weights are located. Weights are ponderation given to each previous node which is used to give the final output. For binary classification is very common to find a sigmoid activation function which can be seen in Fig. 25 and whose formula is given by:

$$f(x) = \frac{1}{1 + e^{-x}} \tag{35}$$

This activation function is used because its result always is between $0$ and $1$ which is the same range in which probability exists [47].

As it can be seen, the result goes from 0 to 1 which has infinite results as there are infinite numbers between 0 and 1. A way to solve this problem is to use the piecewise function:

$$f(u) \begin{cases} 0 & \text{if } u < 0.5 \\ 1 & \text{if } u \geq 0.5 \end{cases} \tag{36}$$

Where $u$ is the result of the sigmoid function.

The result of $f(u)$ is going to be always either 0 or 1. If the result is 0 it means that the binary classification output is class 1 and if the result is 1, it means that the binary classification output is class 2..

The architecture used for the developed CNN for this work, can be seen in Fig. 26. Some of its main features are:

- Array input size of Nx1500x3.

- It has 19 Layers.

- Array output size of Nx1

- Output value between 0 and 1 because its dense layer is activated by a sigmoid function.
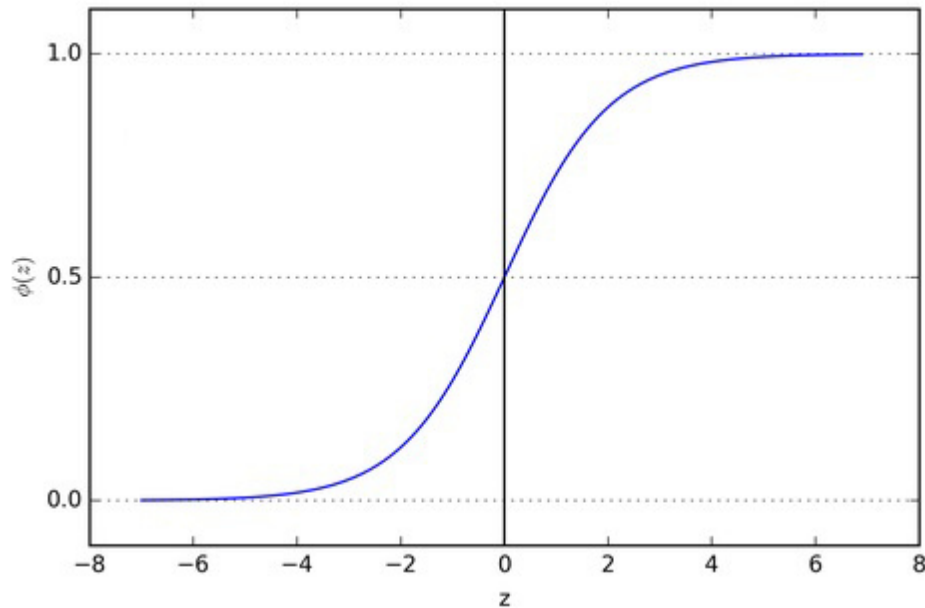
**Figure 25.** Sigmoid activation function [48].

- Uses batch normalization before the activation function which helps to stabilize the training process and improves the final model's performance.

## 5.4. Cost Analysis

In Table 16 it can be seen the cost of developing the project prototype. As it can be seen, the total cost is $1119.5\,\$$. Some of the prototype features are:

- Has a friendly graphic user interface in which the user can select to make a new recording and to show previous recording.

- Recognize if there exists traces of epilepsy patterns by using A.I. with only 2 clicks.

- Can work on any computer as long as the software is installed and the software is easy to install.

- Is portable and has the capacity to store any element in the built-in basket, as well as to have space for a laptop on top of the desk. Also due to its dimensions it fits everywhere and is easy to transport.

- Can adquire brain signals from 10 different monopolar channels.

**Figure 26.** Architecture used for the developed CNN.
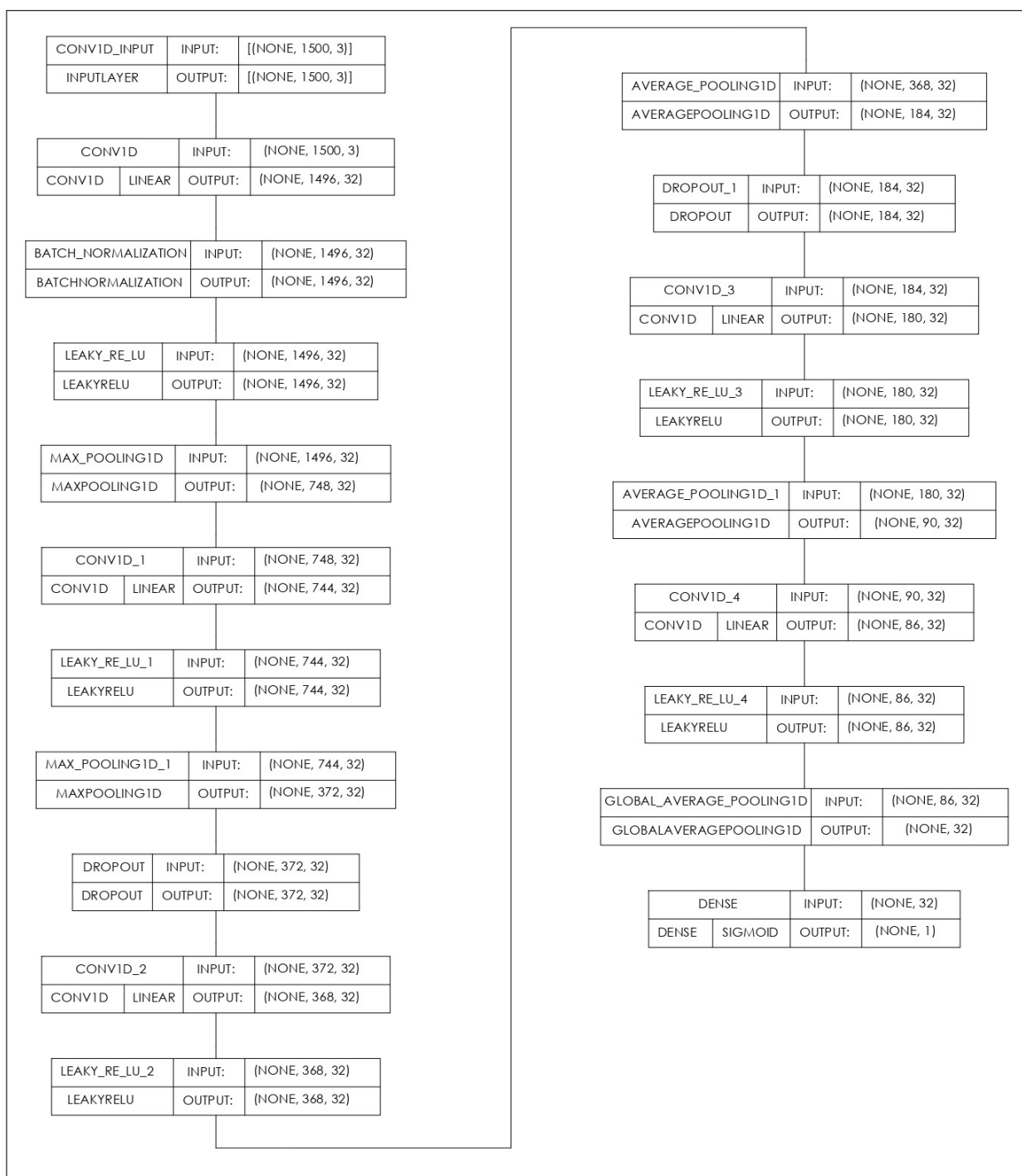
Finally, it is important to highlight that the cost of the $\frac{\text{kW}}{\text{h}}$ in Ecuador is $0.92\,\$$. The total consumption of the prototype can be seen in Table 12. It must be remarked that this table does not contain the cost of the computer in which the software runs because the power a computer uses varies greatly. Therefore an approximate hourly cost of using

**Table 16.** Prototype table of costs.

| Item | Cost $ | Quantity | Total $ |
|---|---|---|---|
| AD620 | 7 | 10 | 70 |
| PIC18F2550 | 10 | 1 | 10 |
| Electrodes | 12 | 12 | 144 |
| 9V Rechargeable | 12 | 2 | 24 |
| PCB | 22.5 | 1 | 22.5 |
| Desk | 170 | 1 | 170 |
| Electronic components | 1 | 10 | 10 |
| 3D Printing | 1 | 50 | 50 |
| Wheels | 1 | 4 | 4 |
| Miscellaneous | 1 | 15 | 15 |
| Design | 600 | 1 | 600 |
| Total | | | 1119.5 |

the prototype is:

$$0.997 \, \text{W} \cdot 0.92 \, \$ \cdot \frac{\text{h}}{\text{kW}} = 0.000\,92 \, \$ \cdot \text{h} \tag{37}$$

# REFERENCES

[1] Made-In-China, "Portable eeg machine." [On-line]. Available: https://www.made-in-china.com/video-channel/sino-med‿cFqJZlLMLukh‿Portable-EEG-Machine-with-Polysomnography.html

[2] Cephalon, "Nicolet eeg." [On-line]. Available: https://www.cephalon.eu/products/eeg-erp/neeg/

[3] W. Data, "Average height of men and women worldwide." [On-line]. Available: https://www.worlddata.info/average-bodyheight.php

[4] C. Height, "Average height in ecuador (men and women)." [On-line]. Available: https://colonelheight.com/average-height-in-ecuador-men-and-women/

[5] H. P. PHD(c), "Desk height calculator: Office ergonomics in a blink." [On-line]. Available: https://www.omnicalculator.com/everyday-life/desk-height

[6] I. Calculator, "Desk height calculator." [On-line]. Available: https://www.inchcalculator.com/desk-height-calculator/

[7] MegaShop, "Hogar y cocina :: Mesa plegable para portátil laptop tablet con porta vaso." [On-line]. Available: https://megashop.com.mx/hogar-cocina/mesa-plegable-para-portatil-laptop-tablet/

[8] T. Oi, "Mesa plegable cama 60x40cm." [On-line]. Available: https://www.tiendaoi.com/producto/mesa-plegable-cama-60x40/

[9] M. D. S. PUBLICA, "Encuesta nacional de salud y nutricion."

[10] G. Wengert, "Examine the value of mdf." [On-line]. Available: https://www.woodworkingnetwork.com/magazine/fdmc-magazine/examine-value-mdf

[11] EngineeringToolbox, "Cantilever beams - moments and deflections." [On-line]. Available: https://www.engineeringtoolbox.com/cantilever-beams-d‿1848.html

[12] Rocscience, "Factor of safety and probability of failure."

[13] L. E. Osgood, G. Cameron, y E. Christensen, "6.2 shear/moment diagrams."

[14] dipac, "Tubo estructural cuadrado negro." [On-line]. Available: https://dipacmanta. com/producto/tubos/tubo-estructural/tubo-estructural-cuadrado-negro/

[15] A. Materials, "Aisi 1008 carbon steel (uns g10080)." [On-line]. Available: https://www.azom.com/article.aspx?ArticleID=6538

[16] Kywi, "Garrucha 40mm 40kg ny.pg.b.l fierro." [On-line]. Available: https: //kywitiendaenlinea.com/product/garrucha-40mm-40kg-ny-pg-b-l-fiero/

[17] E. Deneke, "Wet vs dry: Which electrodes should i choose?" [On-line]. Available: https://www.linkedin.com/pulse/ wet-vs-dry-which-electrodes-should-i-choose-eduard-deneke/

[18] D. Tanner, K. Morgan-Short, y S. J. Luck, "How inappropriate high-pass filters can produce artifactual effects and incorrect conclusions in erp studies of language and cognition," *Psychophysiology*, vol. 52, pp. 997–1009, 2015.

[19] C. S. Nayak y A. C. Anilkumar, "Eeg normal waveforms," *StatPearls*, pp. 1–6, 7 2022. [On-line]. Available: https://www.ncbi.nlm.nih.gov/books/NBK539805/

[20] A. C. N. Society, "American clinical neurophysiology society guideline 8: Guide-lines for recording clinical eeg on digital media 1," 2006.

[21] L. Goncales, "The effects of applying filters on eeg signals for classifying developers' code comprehension," *Redalyc*, 12 2021. [On-line]. Available: https://www.redalyc.org/journal/474/47471710003/html/

[22] B. S. Miller, "Ece senior capstone project analog vs. digital filtering of data."

[23] T. Anwarch, "Eeg epilepsy detection tutorial." [On-line]. Available: https: //github.com/talhaanwarch/youtube-tutorials/blob/main/eeg_epilepsy.ipynb

[24] E. Tutorials, "Passive low pass filter." [On-line]. Available: https://www. electronics-tutorials.ws/filter/filter_2.html

[25] A. Gramfort, M. Luessi, E. Larson, D. A. Engemann, D. Strohmeier, C. Brodbeck, R. Goj, M. Jas, T. Brooks, L. Parkkonen, y M. S. Hämäläinen, "MEG and EEG data analysis with MNE-Python," *Frontiers in Neuroscience*, vol. 7, no. 267, pp. 1–13, 2013.

[26] E. Notes, "Op amp notch filter: Active filter circuit." [On-line]. Available: https://www.electronics-notes.com/articles/analogue_circuits/operational-amplifier-op-amp/notch-filter-active-circuit.php

[27] H. M, "Bandpass filter." [On-line]. Available: https://hossainhere.wordpress.com/2010/07/19/bandpass-filter/

[28] T. Instruments, "Low cost low power instrumentation amplifier ad620 applications weigh scales ecg and medical instrumentation transducer interface data acquisition systems industrial process controls battery-powered and portable equipment connection diagram," 2003. [On-line]. Available: www.analog.com

[29] L. A. Moctezuma y M. Molinas, "Eeg channel-selection method for epileptic-seizure classification based on multi-objective optimization," *Frontiers in Neuroscience*, vol. 14, p. 593, 6 2020. [On-line]. Available: /pmc/articles/PMC7312219//pmc/articles/PMC7312219/?report= abstracthttps://www.ncbi.nlm.nih.gov/pmc/articles/PMC7312219/

[30] V. J. Lawhern, A. J. Solon, N. R. Waytowich, S. M. Gordon, C. P. Hung, y B. J. Lance, "Eegnet: A compact convolutional neural network for eeg-based brain-computer interfaces," *Journal of Neural Engineering*, vol. 15, 7 2018.

[31] L. Pham-Nguyen, V. Nguyen-Thien, T.-D. L. Van, K. Q. Nguyen, y H.-D. Han, "A 5.8- w 61.29-db-sndr 10-bits configurable eeg acquisition system," pp. 199–203, 8 2022.

[32] K. K. Mandrumaka y F. Noorbasha, "A low power 10 bit sar adc with variable threshold technique for biomedical applications," *SN Applied Sciences*, vol. 1, pp. 1–9, 8 2019. [On-line]. Available: https://link.springer.com/article/10.1007/s42452-019-0940-3

[33] G. Wright, "What is the nyquist theorem?" [On-line]. Available: https://www.techtarget.com/whatis/definition/Nyquist-Theorem

[34] Microchip, "Pic18f2455/2550/4455/4550 data sheet," 2006.

[35] R. Pi, "Raspberry pi 4 model b specifications." [On-line]. Available: https://www.raspberrypi.com/products/raspberry-pi-4-model-b/specifications/

[36] Microchip, "Atmega2560." [On-line]. Available: https://www.microchip.com/en-us/product/ATMEGA2560

[37] CADENCE, "Maximum power output and data transfer rates for the usb standards." [On-line]. Available: https://resources.pcb.cadence.com/blog/2020-what-are-the-maximum-power-output-and-data-transfer-rates-for-the-usb-standards

[38] Energizer, "Energizer nh22-175." [On-line]. Available: https://data.energizer.com/pdfs/nh22-175.pdf

[39] G. Van Rossum y F. L. Drake, *Python 3 Reference Manual*. Scotts Valley, CA: CreateSpace, 2009.

[40] M. Roseman, "Modern tkinter for busy python developers : quickly learn to create great looking user interfaces for windows, mac and linux using python's standard gui toolkit," p. 257, 2020.

[41]

[42] X. Pang, Y. Zhou, P. Wang, W. Lin, y V. Chang, "An innovative neural network approach for stock market prediction," *Journal of Supercomputing*, vol. 76, pp. 2098–2118, 3 2020. [On-line]. Available: https://www.investopedia.com/terms/n/neuralnetwork.asp

[43] B. Rohrer, "How do convolutional neural networks work?" [On-line]. Available: https://e2eml.school/how_convolutional_neural_networks_work.html

[44] upGrad, "Neural network: Architecture, components top algorithms." [On-line]. Available: https://www.upgrad.com/blog/neural-network-architecture-components-algorithms/

[45] T. H. Afridi, "A multimodal memes classification: A survey and open research is-sues." [On-line]. Available: https://www.researchgate.net/publication/344294512_A_Multimodal_Memes_Classification_A_Survey_and_Open_Research_Issues

[46] A. Dertat, "Applied deep learning - part 4: Convolutional neural networks." [On-line]. Available: https://towardsdatascience.com/applied-deep-learning-part-4-convolutional-neural-networks-584bc134c1e2

[47] S. SHARMA, "Activation functions in neural networks." [On-line]. Available: https://towardsdatascience.com/activation-functions-neural-networks-1cbd9f8d91d6

[48] W. MathWorld, "Sigmoid function." [On-line]. Available: https://mathworld.wolfram.com/SigmoidFunction.html